

Resonant Absorption of Neutrons by Crystals*

H. E. JACKSON AND J. E. LYNN†
Argonne National Laboratory, Argonne, Illinois

(Received March 7, 1962)

A study has been made of the Doppler broadening of resonances in the total cross section for interaction of slow neutrons with nuclei bound in crystals. The resonance at 6.71 eV in Os metal and the resonance at 6.65 eV in U metal were chosen as examples of moderate crystal binding, while the 6.65-eV resonance in U_3O_8 , for which $k\theta_0=0.043$ eV, was chosen as an example of strong binding. The shapes of the resonance lines were determined as a function of temperature by measuring the neutron transmission of thin and thick samples by means of the Argonne fast chopper. These shapes were compared with theoretical line shapes calculated by means of Lamb's theory of Doppler broadening as applied to the spectra of lattice frequencies implied by simple models of the crystal lattices. For moderate binding, a simple Einstein model which reproduces the observed specific-heat behavior of the crystal above 40°K gives accurate resonance-line shapes at all temperatures. However, for U_3O_8 the line shape implies a generalized Nernst-Lindemann model of the lattice with a frequency spectrum $g(\nu)=0.9\delta(\hbar\nu_1-0.013\text{ eV})+0.1\delta(\hbar\nu_2-0.052\text{ eV})$. The proportions of the high- and low-frequency components are quite different from the values resulting from specific-heat data. Possible interpretations of the U_3O_8 results in terms of simple lattice models are presented.

I. INTRODUCTION

THE standard expression for the description of a slow-neutron resonance cross section is the single-level Breit-Wigner formula. It describes the purely nuclear effect on the cross section, and its main energy variation is contained in the factor

$$B(E)=1/(E-E_R)^2+(\frac{1}{2}\Gamma)^2. \quad (1)$$

Here, E_R is the virtual energy level of the compound nucleus (neutron+target) which is responsible for the occurrence of the resonance, Γ is the resonance width, which is inversely proportional to the lifetime of the virtual level, and E is the energy available for excitation of the compound nucleus. In neutron spectroscopy, however, the neutron kinetic energy in the laboratory system, E_n , is the quantity measured and so the resonance cross section must be known as a function of neutron laboratory energy. This is simple if the target nucleus is free and at rest for E is then the neutron energy E_n diminished by the recoil energy $R=mE_n/(M+m)$ of the compound nucleus, m and M being the masses of the neutron and target nuclei, respectively.

In practice, the thermal motions of the target nuclei in the sample being studied are usually an important consideration. Only in the cross sections at the broad resonances characteristic of light nuclei may the thermal modification of the resonance shape be neglected. The discussion of the usual case follows most easily after introducing an energy transfer E_t defined as the difference between E_n and E , and an energy-transfer function $S(E_t)$ which is convoluted with the Breit-Wigner term $B(E)$ in Eq. (1) to obtain the cross section as a function of neutron energy. The latter function, denoted here by $W(E_n)$, is usually known as the

"Doppler broadened" resonance form and is given by

$$W(E_n)=\int dE_t S(E_t)B(E_n-E_t). \quad (2)$$

In calculating resonance broadening, the assembly of target nuclei is commonly treated as a perfect gas.^{1,2} In this model, the energy transfer is approximately

$$E_t \approx R + mvw_x, \quad (3)$$

where v is the neutron velocity in the laboratory system and w_x is the velocity of the target nucleus in the direction of the neutron beam. The Ψ function, familiar in neutron spectroscopy, is obtained for the resonance shape after applying the Maxwell-Boltzmann formula for the distribution of velocities w_x in a gas at temperature T :

$$S(E_t)=(1/\Delta\sqrt{\pi})\exp[-(E_t-R)^2/\Delta^2], \quad (4)$$

$$\Psi(E_n)=W(E_n),$$

where $\Delta=(4RkT)^{1/2}$, k being Boltzmann's constant. The same result holds for a classical solid in which the target nuclei are treated as harmonic oscillators whose energies are governed by Boltzmann statistics.

A theoretical study of the resonance shape that would result for target nuclei bound in a quantum-mechanical crystal was made by Lamb many years ago.³ The quantum-mechanical behavior of a crystal affects the resonance cross section in ways that are not apparent from a study of classical systems. A simple qualitative discussion of the quantum effects may be pursued in terms of a target nucleus bound in a harmonic-oscillator well. If the nucleus is initially at rest, then in the classical model the coalescing neutron will give it a recoil energy R and the compound system will oscillate in the well with this energy. The resonance then has the

* Work performed under the auspices of the U. S. Atomic Energy Commission.

† On leave from the Atomic Energy Research Establishment, Harwell, Berkshire, England.

¹ H. A. Bethe and G. Placzek, Phys. Rev. **51**, 462 (1937).

² H. A. Bethe, Revs. Modern Phys. **9**, 140 (1937).

³ W. E. Lamb, Phys. Rev. **55**, 190 (1939).

Breit-Wigner shape, corresponding to zero temperature in Eq. (4). In the quantum-mechanical model, on the other hand, the energy of oscillation will be one of the eigenvalues of the harmonic-oscillator well, any given eigenvalue appearing with a characteristic probability. The expectation value of this energy is equal to the recoil energy R . In particular, there will be a finite probability of the oscillator remaining in its initial state. This is the analog of the Mössbauer effect of recoilless absorption of nuclear gamma rays.⁴ In addition to this sharp Breit-Wigner shape at neutron energy E_R , there will be fine structure (or general broadening if Γ is greater than the spacing of eigenvalues in the oscillator well) at adjacent neutron energies so that the "Mössbauer line" may be obscured.

The modes of oscillation in a crystal are to be considered as a property of the lattice as a whole rather than as residing on individual atoms, but the main qualitative conclusions are similar to those stated above. Lamb derived expressions for the probability of creation or annihilation of quanta (phonons) in the various modes of oscillation and used these in an explicit calculation of the resonance shape to be expected if the target nuclei were bound in a Debye crystal. For a cold crystal (relative to the Debye temperature Θ_D), and for a sufficiently small neutron resonance width and a fairly low recoil energy (both compared with $k\Theta_D$), he showed that a "recoilless" Breit-Wigner peak could be expected, as well as some crude structure at higher energies. At higher crystal temperatures the usual result is the classical resonance broadening, except that the classical mean energy per degree of freedom, kT , in Eq. (4) must be replaced by the quantum-mechanical mean energy,

$$\bar{\epsilon} = \frac{1}{2} \int_0^{\nu_m} d\nu h\nu \coth(h\nu/2kT) g(\nu), \quad (5)$$

where $g(\nu)$ is the spectrum of oscillation modes of the lattice, and ν_m is the maximum frequency of this spectrum. The mean energy $\bar{\epsilon}$ is greater than kT but approaches it asymptotically in the high-temperature limit.

Lamb's classical form of resonance broadening has found common use in neutron spectroscopy. An experimental verification of this form was made by Landon in a measurement of the 1.26-eV resonance in the rhodium cross section.⁵ Recent improvements in the intensity and in the instrumental resolution of neutron spectrometers have made an examination of the deviations from the classical approximation feasible through the study of narrower resonances. The incentive for such a study has been enhanced, of course, by the discovery of the Mössbauer effect, to which Lamb's

theory is almost directly applicable. The aims are twofold. First, there is the practical value to neutron spectroscopy; the conditions under which crystal effects may be discerned in the resonance shape and the models by which they may be explained and which may also be used to derive nuclear resonance parameters from cross-section measurements are of particular interest to workers in this field. Second, there is the possibility of learning something about the lattice dynamics through experiments of this kind; a narrow resonance, whose nuclear parameters are known, may be regarded as a probe for measuring some features of the lattice oscillation spectrum $g(\nu)$.

In this paper we present an account of an experiment in which we have studied the Doppler broadening of resonances at 6.65 eV in the cross section of U^{238} and at 6.71 eV in the cross section of Os^{189} under varying conditions of crystal binding. A preliminary account of early phases of the work has already been reported.⁶ The osmium resonance was studied in a metallic sample. The appropriate parameters,⁷ $\Gamma=0.087$ eV, $k\Theta_D=0.024$ eV, are typical of a case of weak binding for which Lamb's classical form of broadening should be appropriate. Absorption by the uranium resonance for which $\Gamma=0.028$ eV and $R=0.028$ eV was studied in samples of two different compositions. A metallic foil of natural uranium was used as an example of moderate binding. A sample of U_3O_8 was expected to be an example of strong binding. According to available specific-heat data,^{8,9} the Debye "temperatures" of these two samples are 0.014 and 0.043 eV, respectively. The temperature dependence of the line shape was studied for all of these samples. The measurements and resolution corrections are described in Sec. II. In Sec. III, Lamb's basic formalism is used to analyze the data in terms of crude crystal models, and the significance of our results is considered in Sec. IV.

II. EXPERIMENTAL PROCEDURE

The total cross sections in the region of the resonances studied were determined by transmission measurements made with the Argonne fast chopper¹⁰ operated with a flight path of 58.9 m. The half width of the time-of-flight resolution function of the system was $0.038 \mu\text{sec/m}$, which corresponds to an energy spread of 0.018 eV at 6.7 eV. The background counting rate was continuously monitored by passing the neutron beam through filters

⁶ H. E. Jackson, L. M. Bollinger, and R. E. Coté, *Phys. Rev. Letters* **6**, 187 (1961).

⁷ M. W. Holm, U. S. Atomic Energy Commission Research and Development Report IDO-16399, 1957 (unpublished).

⁸ J. J. Katz and E. Rabinowitch, *The Chemistry of Uranium* (McGraw-Hill Book Company, Inc., New York, 1951), Chap. 11, p. 271.

⁹ E. F. Westrum, Jr. and F. Grønvald, *J. Am. Chem. Soc.* **81**, 1777 (1959).

¹⁰ L. M. Bollinger, R. E. Coté, and G. E. Thomas, *Proceedings of the Second International Conference on the Peaceful Uses of Atomic Energy, Geneva, 1958* (United Nations, Geneva, 1958), Vol. 14, p. 239.

⁴ R. L. Mössbauer, *Z. Physik* **151**, 124 (1958); *Naturwissenschaften* **45**, 538 (1958).

⁵ H. H. Landon, *Phys. Rev.* **94**, 1215 (1954).

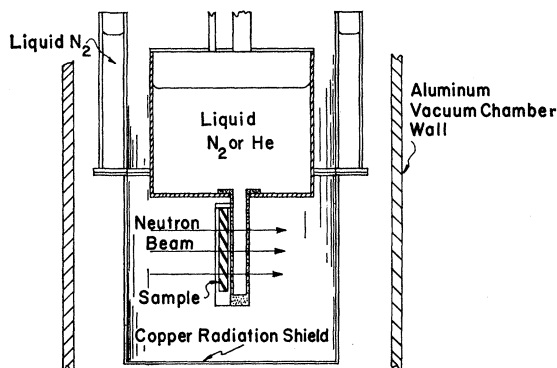


FIG. 1. Liquid helium cryostat. The volume within the aluminum walls is pumped to a pressure of 10^{-6} mm Hg. The liquid helium reservoir is connected to the top of vacuum chamber by thin-walled stainless steel filling tubes 14-in. long.

of platinum and silver which were thick enough to remove all timed neutrons in the neighborhood of the resonances at 11.9 and 5.2 eV. Our results indicated that the background rate decreased 10% between 11.9 and 5.2 eV and that the signal-to-background ratio was 6:1 at 6.65 eV. Measurements in which a thick sample of uranium was used indicated that the energy-dependent component of the background was well approximated by a linear variation.

Resonance energies and approximate resonance parameters were determined from measurements of the metallic samples of uranium and osmium at room temperature by fitting the data to theoretical curves. As expected from the foregoing discussion, the gas model was completely adequate for analysis of these data. This was indicated by the acceptable values of χ^2 obtained for fits to the curves drawn for the best values of the parameters. In subsequent measurements made at 77 and 4°K, the time of flight in the region of 6.7 eV was measured relative to peak positions of the sharp resonance in platinum at 19.4 eV. The position of the peak could be determined to within 0.1 channel width (0.1 μ sec). The total drift in the system was less than 0.1 channel in any 24-h period. Thus, any displacement of features of the line shapes at 6.7 eV relative to the resonance in platinum must be interpreted as characteristic of Doppler broadening by the crystal structure of the sample under study.

Measurements of the osmium sample were made with a cryostat which is in every respect similar to the design used by Landon.⁵ However, the uranium samples were cooled in a cryostat of more elaborate design shown schematically in Fig. 1. The reservoir for liquid helium or nitrogen was a thin-walled stainless cylinder to which the hollow copper sample plate was soldered. The sample holder was clamped directly to this plate. A small temperature difference between the sample and the reservoir was insured by the presence of the liquid directly behind the sample. The entire region surrounding the sample and radiation shield was evacuated to a

pressure of 10^{-6} mm Hg. The transmission of the cryostat, including the aluminum walls of the vacuum chamber without the sample in place, was approximately 0.8 and was constant over the time-of-flight region of interest.

Because of the detailed nature of the comparison between our measured values and the predictions of various models, a correction for the effect of instrumental resolution was required. The maximum correction of 6% was required for the measurements of metallic uranium at 4°K. Consequently, a satisfactory correction was obtained from the formula of Seidl *et al.*,¹¹ namely,

$$T_{\text{true}}(t) = T_{\text{obs}}(t) - \frac{1}{2} T_{\text{obs}}''(t) \int_{-\infty}^{\infty} (t-t')^2 R(t,t') dt' - \frac{T_{\text{obs}}^{(4)}(t)}{4!} \left[\int_{-\infty}^{\infty} (t-t')^4 R(t,t') dt - 6 \left(\int_{-\infty}^{\infty} (t-t')^2 R(t,t') dt \right)^2 \right], \quad (6)$$

where T_{obs} is the observed transmission, $R(t,t')$ is the experimental resolution function, and t is the time of flight. The experimental data were fitted by the method of least squares to a polynomial in t which was then used as $T_{\text{obs}}(t)$ in Eq. (4) to determine the correction to be applied to each point of the measured transmission dip. All data presented in this paper have been corrected in this manner. It should be noted that any details of the resonance shapes whose structure is smaller than the resolution width will not be revealed by this correction.

III. ANALYSIS OF RESULTS

The complete equation for the total cross section near an isolated absorption resonance is

$$\sigma(E_n) = \pi \lambda^2 g_J \Gamma_n \Gamma W(E_n), \quad (7)$$

where Γ_n is the neutron width of the resonance, g_J is a statistical factor depending on the angular momentum $J\hbar$ of the virtual level, and λ is the de Broglie wavelength (divided by 2π) corresponding to the relative motion of neutron and nucleus. Notice that λ , Γ_n , and Γ all depend mildly on the energy E available for excitation of the compound nucleus. These energy dependences will not be described explicitly here but have been taken into account in our calculations, as was a small term (representing the interference between potential scattering and the resonance) which was neglected in Eq. (7).

The general form of $W(E_n)$ which Lamb obtained

¹¹ F. G. P. Seidl, D. J. Hughes, H. Palevsky, J. S. Levin, W. Y. Kato, and N. G. Sjöstrand, Phys. Rev. **95**, 476 (1954).

from dispersion theory is

$$W(E_n) = \sum_{\{\alpha_s\}} \rho\{\alpha_s\} \times \sum_{\{n_s\}} \frac{|\langle \{n_s\} | \exp(i\mathbf{p} \cdot \mathbf{x}_L/\hbar) | \{\alpha_s\} \rangle|^2}{[E_n - E_R - \sum_s (n_s - \alpha_s) h\nu_s]^2 + (\frac{1}{2}\Gamma)^2}. \quad (8)$$

This expression describes the collision of a neutron of laboratory energy E_n and momentum \mathbf{p} with the L th atom, whose coordinates are \mathbf{x}_L , bound in a medium whose initial quantum numbers are the set $\{\alpha_s\}$ and whose intermediate quantum numbers (after formation but before decay) are the set $\{n_s\}$. The subscript s refers to the modes of oscillation and the numbers α_s and n_s refer to the numbers of quanta of frequencies ν_s in the modes s . The quantity $\rho\{\alpha_s\}$ is the Boltzmann weighting factor for the states $\{\alpha_s\}$ when the sample is at temperature T .

Clearly the energy-transfer function corresponding to Eq. (8) is

$$S(E_t) = \sum_{\{\alpha_s\}} \rho\{\alpha_s\} \sum_{\{n_s\}} |\langle \{n_s\} | \exp(i\mathbf{p} \cdot \mathbf{x}_L/\hbar) | \{\alpha_s\} \rangle|^2 \times \delta[E_t - \sum_s (n_s - \alpha_s) h\nu_s]. \quad (9)$$

Lamb's expressions for evaluating the matrix elements in Eq. (9) are:

$$\langle \{n_s\} | \exp(i\mathbf{p} \cdot \mathbf{x}_L/\hbar) | \{\alpha_s\} \rangle = \prod_s K(n_s, \alpha_s; q_s), \quad (10a)$$

$$q_s^2 = (\mathbf{p} \cdot \mathbf{e}_s)^2 / 2Mh\nu_s N, \quad (10b)$$

$$|K(\alpha_s, \alpha_s; q_s)|^2 = (1 - 2\alpha_s q_s^2) e^{-q_s^2}, \quad (10c)$$

$$|K(\alpha_s + 1, \alpha_s; q_s)|^2 = (\alpha_s + 1) q_s^2 e^{-q_s^2}, \quad (10d)$$

$$|K(\alpha_s - 1, \alpha_s; q_s)|^2 = \alpha_s q_s^2 e^{-q_s^2}, \quad (10e)$$

where \mathbf{e}_s is the polarization vector of a wave in the mode s . The K 's involving annihilation or creation of more than one phonon in a particular mode s may be neglected because they are of higher order in q_s^2 , which is inversely proportional to the large number N of atoms in the fundamental volume of the crystal. If the crystal is isotropic, averaging over \mathbf{e}_s for a given frequency ν_s leads to $q_s^2 = R/(h\nu_s 3N)$. After making this assumption, the calculation may proceed in terms of the frequency distribution $g(\nu)$. If the crystal is not isotropic, then it would be necessary to carry out the calculations in terms of the distribution of q_s^2 and then average over the random orientation of crystallite directions within the sample. In view of the facts that nothing precise is known about the polarizations of phonons in the materials we are investigating and that our measurements are unlikely to be sensitive to all these characteristics of the phonons, we have assumed isotropy in analyzing the data. Presumably there would be little difference, at least qualitatively, in the results obtained if it were possible to proceed in the other way. The isotropy assumption is in any case in accord with the spirit of the crude crystal models employed in this paper.

It is easy to show by use of Eqs. (10) that the energy-transfer function may be expanded in the form

$$S(E_t) = \exp \left[- \sum_s \coth \left(\frac{h\nu_s}{2kT} \right) q_s^2 \right] \left[\delta(E_t) + \sum_s \frac{q_s^2}{1 - e^{-h\nu_s/kT}} \delta(E_t - h\nu_s) + \sum_s \frac{q_s^2}{e^{h\nu_s/kT} - 1} \delta(E_t + h\nu_s) \right. \\ \left. + \sum_{s,t} \frac{q_s^2 q_t^2 \delta(E_t - h\nu_s - h\nu_t)}{(1 - e^{-h\nu_s/kT})(1 - e^{-h\nu_t/kT})} + 2 \sum_{s,t} \frac{q_s^2 q_t^2}{(1 - e^{-h\nu_s/kT})(e^{h\nu_t/kT} - 1)} \delta(E_t - h\nu_s + h\nu_t) \right. \\ \left. = \sum_{s,t} \frac{q_s^2 q_t^2}{(e^{h\nu_s/kT} - 1)(e^{h\nu_t/kT} - 1)} \delta(E_t + h\nu_s + h\nu_t) + \dots \right]. \quad (11)$$

Then making the isotropy assumption and using the spectrum of frequencies, $g(\nu)$ leads to

$$S(E_t) = \exp \left(- R \int_0^{\nu_m} d\nu \frac{g(\nu) \coth(h\nu/2kT)}{h\nu} \right) \left(\delta(E_t) + R \frac{g(|E_t|/h)}{|E_t| (1 - e^{-|E_t|/kT})} \right. \\ \left. + \frac{R^2}{2!} \int_{-\infty}^{\infty} d\nu \frac{g(|\nu|) g[|(E_t/h) - \nu|]}{|h\nu| (1 - e^{-h\nu/kT}) |h[(E_t/h) - \nu]| (1 - e^{-(E_t - h\nu)/kT})} + \frac{R^3}{3!} \int_{-\infty}^{\infty} d\nu \frac{g[|(E_t/h) - \nu|]}{|(E_t - h\nu)| (1 - e^{-(E_t - h\nu)/kT})} \right. \\ \left. \times \int_{-\infty}^{\infty} d\nu' \frac{g(|\nu'|) g(|\nu - \nu'|)}{|h\nu'| (1 - e^{-h\nu'/kT}) |h\nu - h\nu'| (1 - e^{-h(\nu - \nu')/kT})} + \dots \right). \quad (12)$$

From Eq. (12), $S(E_t)$ may be computed in a straightforward manner for various models of the spectrum $g(\nu)$. The results are then used to calculate $W(E_n)$,

which may be compared by the least-squares method with the experimental data.

An alternative approach, which is more general and

extracts the maximum amount of information, involves determining the moments of $S(E_i)$ from the experimental data. A general consideration of this approach will be deferred to a later paper. However, we cite two results of particular relevance to the present discussion. By applying statistical methods, the first and second moments of $S(E_i)$ can be shown to be related to those of the frequency spectrum $g(\nu)$ of the lattice through the expressions

$$\bar{E}_i = R, \quad (13a)$$

$$\langle E_i^2 \rangle_{av} = R^2 + R\langle h\nu \rangle, \quad (13b)$$

where $\langle h\nu \rangle$ is defined as

$$\langle h\nu \rangle = \int_0^{\nu_m} d\nu g(\nu) h\nu \coth(h\nu/2kT) = 2\bar{\epsilon}. \quad (13c)$$

Here, $\coth(h\nu_s/2kT)$ represents the mean occupation number of the ν_s mode at temperature T . The first relation is merely a statement of Lipkin's sum rule¹² for Mössbauer radiation, namely, the mean energy transferred to the lattice is independent of the lattice model. The second moment, according to Eq. (13b), depends only on the mean energy, i.e., on the first moment of the phonon excitation spectrum at the temperature of the sample. In the discussion of our results, therefore, we have regarded lattice models to be equivalent if their mean energies at a given temperature are equal. It should be noted that Lamb's effective-temperature approximation is merely the substitution of a classical assembly whose temperature is determined by the requirement that the mean energy, and consequently the second moment of $S(E_i)$, should be equal to that of the lattice it replaces.

The structure of the function $S(E_i)$ will be related to the frequency spectrum of the crystal lattice under study. Presumably, one cannot study $S(E_i)$ in any detail with a resolution function that has a much greater width than the maximum $h\nu_m$ of the frequency spectrum itself, without smoothing out the features of $S(E_i)$ caused by the particular lattice. The approximate value of $h\nu_m$ for a particular case can be obtained from specific-heat data. Because the Breit-Wigner shape of the resonance line is the resolution function for this experiment, the resonance parameters can then be related to the degree of detail required in the frequency spectrum to calculate an accurate line shape. For Os metal the effective Debye temperature of 250°K gives a maximum phonon energy of 0.024 eV compared with a resonance width of 0.086 eV for the resonance at 6.7 eV. Similarly, for U metal, the effective Debye temperature of 165°K gives a maximum phonon energy of 0.014 eV compared with a width of 0.028 eV for the resonance at 6.65 eV. For both these cases, then, a simple approximation, namely, an Einstein model of the lattice, is expected to be sufficient for calculating

the line shape. For U_3O_8 , on the other hand, the specific-heat data imply a frequency spectrum whose maximum is at 0.043 eV; and a simple Einstein model is not adequate. Nevertheless, it is clear that only gross features of the particular lattices studied are important and, consequently, when the Einstein spectrum was not adequate, we used a generalized Nernst-Lindemann model in our computations.

The energies and total resonance widths of the resonances were determined from the data taken at room temperature with the metallic samples by fitting them to the theoretical curves. The data taken at all temperatures were then simultaneously fitted in a least-squares procedure to the calculations on either an Einstein or a generalized Nernst-Lindemann model in which both the characteristic parameters and the neutron width are taken as free parameters. In the Einstein model, the frequency spectrum $g(\nu)$ is given by

$$g(\nu) = \delta(\nu - \nu_E).$$

Substituting $g(\nu)$ into Eq. (12) gives

$$S(E_i) = \exp[-(R/h\nu_E) \coth(h\nu_E/2kT)] \times \sum_{n=-\infty}^{\infty} \delta(E_i - h\nu_E) e^{nh\nu_E/2kT} I_{|n|} \left[\frac{R}{h\nu_E \sinh(h\nu_E/2kT)} \right], \quad (14)$$

where the $I_{|n|}$ are Bessel functions of the first kind with pure imaginary argument. In this case, the calculation of the line shape of a given set of parameters is relatively simple. If the Einstein fit was not adequate, the analysis was then repeated for a generalized Nernst-Lindemann spectrum of the form

$$g(\nu) = a_1 \delta(E_1 - h\nu) + a_2 \delta(E_2 - h\nu); \quad a_1 + a_2 = 1. \quad (15)$$

In this case, $S(E_i)$ was evaluated directly from Eq. (12) by a numerical calculation. Each choice of parameters was used to calculate and sum the terms of Eq. (14) for a sufficient number of values of E_i to permit a numerical integration of Eq. (2) and hence to calculate $\sigma(E_n)$ from Eq. (7). The results for the best fits are shown in Figs. 2, 3, and 5, together with the experimental results which we shall discuss in the following paragraphs.

Osmium

Measurements of the transmission of a powdered sample of metallic osmium with a thickness of 0.00124 atoms/b were made at 297 and 105°K. The results are shown in Fig. 2. These data were fitted very well by a simple Einstein model with $h\nu_E = 0.016$ eV and resonance parameters $\Gamma_n^0 = (1.32 \pm 0.02) \times 10^{-3}$ eV, $\Gamma = (87 \pm 2) \times 10^{-3}$ eV, and $E_R = 6.71$ eV. This value for $h\nu_E$ is also implied by the specific-heat data for osmium. However, the predictions of Lamb's effective-temperature model are not significantly different from the crystal calculation and also give a satisfactory fit within

¹² H. J. Lipkin, Ann. Phys. 9, 332 (1960).

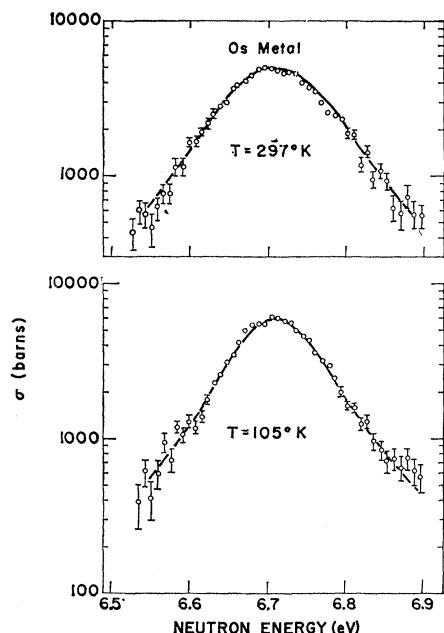


FIG. 2. Measured line shapes for the resonance at 6.71 eV in Os metal at temperatures of 297 and 105°K. The solid curve represents the prediction of a simple Einstein model with $h\nu_E = 0.016$ eV

the accuracy of this experiment. Thus, we may regard osmium metal as an example of weak binding for which Lamb's theory is adequate.

Uranium Metal

The measurements on uranium metal were made with two foils, the thin one having a thickness of 1.40×10^{-4}

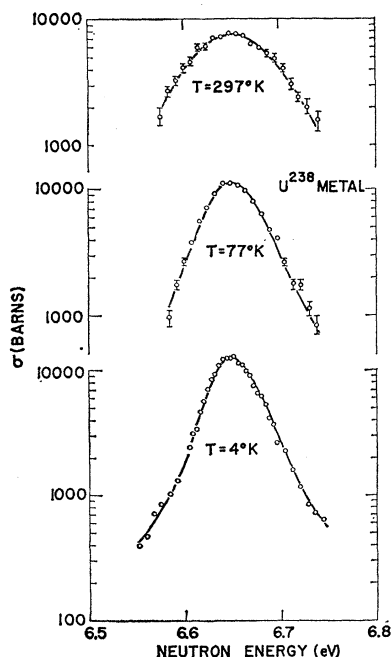


FIG. 3. Measured line shapes for the resonance at 6.65 eV in U metal at temperatures of 297, 77, and 4°K. The solid curve represents the prediction of a simple Einstein model with $h\nu_E = 0.011$ eV.

atoms/b and the thick one 9.53×10^{-4} atoms/b. The results for sample temperatures of 293, 77, and 4°K are shown in Fig. 3, together with the best calculated line shape. The best values of the parameters implied by our results were $h\nu_E = 0.011 \pm 0.002$ eV, $\Gamma_n = (5.90 \pm 0.05) \times 10^{-4}$ eV, and $\Gamma = 0.0285 \pm 0.0015$ eV. Again, the value of $h\nu_E$ is in good agreement with the specific-heat data for metallic uranium, which also gives $h\nu_E = 0.011$ eV. Calculations of the line shape for an equivalent Debye frequency spectrum were also made by using the asymptotic expansion of Nelkin and Parks.¹³ However, the difference between the two shapes was not significant enough to warrant comment.

In Fig. 4, the results for a sample temperature of 4°K have been plotted in detail in order to compare the effective-temperature approximation with the prediction of the crystal model. The fact that the measured points are displaced toward lower energies

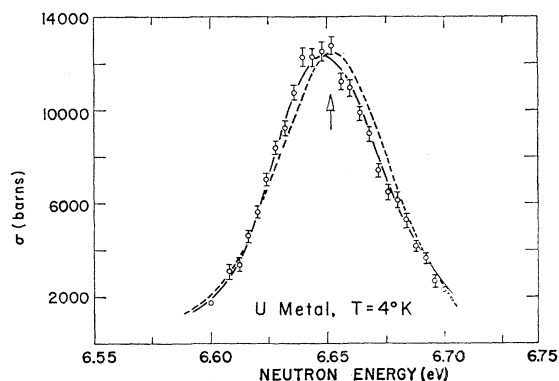


FIG. 4. Measured line shape at 4°K for the 6.65-eV resonance in U metal. The solid curve represents the prediction of a simple Einstein model with $h\nu_E = 0.011$ eV, while the dotted curve represents that of an equivalent "effective temperature" model.

relative to the resonance energy indicates that an appreciable fraction of the captures in the metal occur with only a small number of phonon transfers. The results are not consistent with the effective-temperature approximation but are fitted well by an Einstein model.

U₃O₈

Samples of U₃O₈ of thickness 0.938×10^{-4} atoms/b and 0.889×10^{-3} atoms/b were studied at 293, 77, and 4°K. The results, corrected for resolution, could not be brought into agreement with any Einstein model in which reasonable resonance parameters were used. However, a generalized Nernst-Lindemann model with $a_1 = 0.9$, $h\nu_1 = 0.013$ eV, $a_2 = 0.1$, and $h\nu_2 = 0.052$ eV gave the excellent fit to the data shown by the heavy curve in Fig. 5. With regard to the significance of these parameters, the calculated line shapes were unacceptable for parameters outside the ranges of values:

$$a_1 = 0.90 \pm 0.05, \quad h\nu_1 = 0.013 \pm 0.003,$$

¹³ M. Nelkins and D. E. Parks, Phys. Rev. 119, 1060 (1960).

and

$$h\nu_2 = 0.052 \pm 0.008.$$

In Fig. 6 the data at 4°K are plotted linearly together with the best calculated line shape and an equivalent "pseudo-Einstein model," i.e., a frequency spectrum with two equally weighted frequencies which are separated by an energy interval wide enough to wash out oscillations that would be present in the line shape for a pure Einstein model. The discrepancy between theory and experiment is clear for the latter case and offers convincing evidence for the necessity to use a more detailed model.

IV. CONCLUSIONS AND DISCUSSION

The analysis of our experimental data has revealed some crude features of the vibration spectra of neutron-capturing atoms in the crystal lattice. It is pertinent to compare this information with the results of specific-heat measurements.

It was recorded in the previous section that, for metallic uranium, a simple Einstein model which reproduces the observed specific-heat behavior⁸ above about 40°K is adequate¹⁴ for calculating the resonance shape at all temperatures. As the temperature increases, the detail of the model becomes unimportant until, at room temperature, an effective-temperature model is adequate. This is consistent with Lamb's theory for cases characterized as "weak binding" by the condition that $\Gamma + \Delta \gg 2k\Theta_D$. The osmium data are also consistent with Lamb's theory and with the gross features of the frequency function implied by specific heat data.⁷

The results for U_3O_8 are not so easily explained. There is some question whether the specific-heat data are relevant at all, inasmuch as the neutron absorption process initially excites the vibration of uranium atoms in the U_3O_8 lattice while the specific heat is a manifestation of the uniform excitation of the whole lattice. The frequency spectrum we obtain from the neutron absorption experiments is quite unlike the spectrum that would be inferred from the specific-heat measurements on U_3O_8 .⁹ If the frequency employed for the latter is the same as that determined from the absorption experiments, then the strengths of the low- and high-frequency groups are about 0.4 and 0.6, respectively.

These figures are not unique and the specific-heat data can be reproduced by the spectrum $a_1=0.27$, $h\nu_1=0.009$ eV, $a_2=0.73$, $h\nu_2=0.045$ eV, for example. This set of numbers suggests that the low-frequency group is associated with the uranium atoms and the high-frequency group with the oxygen atoms, the ratio a_1/a_2 being identical with the ratio of relative numbers of uranium and oxygen atoms per unit cell of the lattice. Irrespective of interpretation, however, it is clear that a much stronger high-frequency group is

¹⁴ The simple Einstein model will not, of course, explain the specific-heat data at very low temperatures; the Debye model is necessary for this.

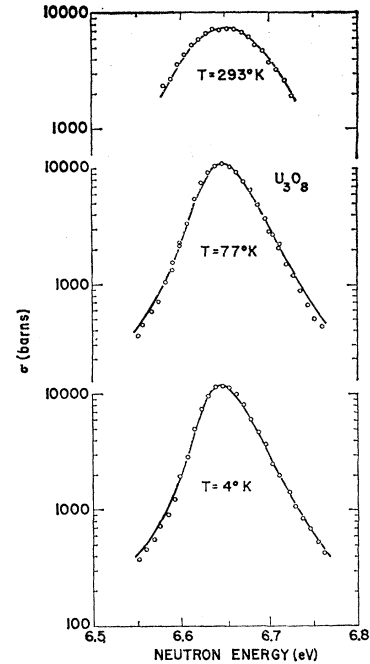


FIG. 5. Measured line shapes for the resonance at 6.65 eV in U_3O_8 at temperatures of 297, 77, and 4°K. The solid curve represents the prediction of a generalized Nernst-Lindemann model with a lattice frequency spectrum $g(\nu) = 0.9\delta(h\nu_1 - 0.013 \text{ eV}) + 0.1\delta(h\nu_2 - 0.052 \text{ eV})$.

necessary to explain the specific heat than is required for the resonance shape. As a striking illustration of this, the line shape that would result from the assumption of the second specific-heat spectrum described above is shown by the dashed line in Fig. 6. Even at room temperatures (not shown here), the specific-heat spectrum gives a resonance shape quite different from the observations.

It is tempting to explain the discrepancy between the two inferred spectra by a naive picture of the U_3O_8 lattice as two virtually independent interpenetrating lattices of uranium and oxygen. The specific heat might not depend drastically on the degree of coupling between

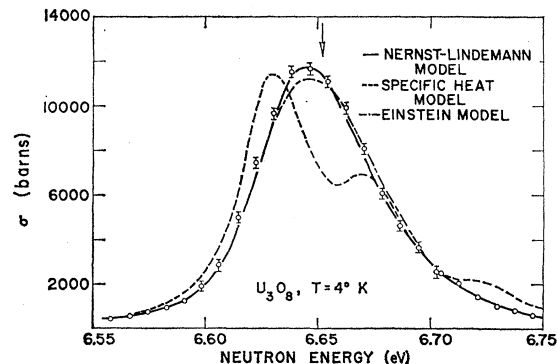


FIG. 6. Measured line shape at 4°K for the 6.65-eV resonance in U_3O_8 . The prediction of the generalized Nernst-Lindemann model of Fig. 5 (solid curve) is compared with the line shape appropriate to the lattice frequency spectrum obtained from specific-heat data. Also shown is the shape for a "pseudo-Einstein model," i.e., a phonon spectrum with two equally weighted frequencies which are separated by an energy interval wide enough to wash out oscillations that would be present for a pure Einstein model.

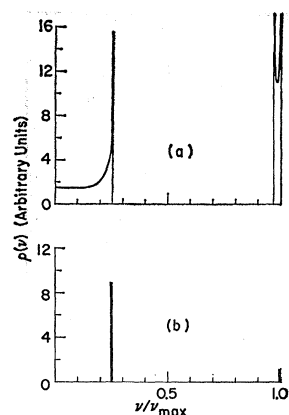


FIG. 7. (a) Spectrum of allowed frequencies in U_3O_8 predicted by linear chain theory. The peaks in the distribution represent infinities in the actual distribution. (b) Spectrum of allowed frequencies used to obtain a "best fit" to the experimental data.

these, but the amount of high-frequency component present in the frequency spectrum governing the uranium resonance shape would be expected to be very sensitive to this coupling.

An alternative explanation can be found by comparing our spectrum with the results of simple linear chain theory.¹⁵ If equally spaced sites on a linear lattice are occupied alternately by particles of mass M and m ($M > m$) and the force F between each pair of neighbors is constant, the resulting spectrum for transverse displacements of the particles has the form shown in Fig. 7a. The maximum frequency of the acoustic branch (low-frequency branch) corresponds to a mode in which alternate particles of mass M differ in phase by π while the particles of mass m are at the nodes of the wave. The high-frequency limit of the optical branch corresponds to a mode in which the neighbors of the chain are in antiphase. Both these modes can be excited by selective neutron absorption by the mass- M particles. On the other hand, in the low-frequency optical mode [which is still higher than the maximum acoustic frequency by a factor $(M/m)^{1/2}$], the heavy particles are at nodal positions. Consequently, this mode will not be excited by selective heavy-particle neutron absorption. In other words, the over-all prob-

ability of excitation of the optical modes is lower than may be expected from a knowledge only of the vibration spectrum. It seems reasonable to assume that these qualitative features of the linear chain will appear in the realistic three-dimensional case. As shown in Fig. 7, the relative frequencies of our spectrum are remarkably close to the frequencies of these modes. Our data imply a small coupling of capture by particles with mass M to the high-frequency mode.

It is interesting to note here that an analogous effect has been observed in this laboratory by Schiffer *et al.*¹⁶ A small amount of Co^{57} was introduced as an impurity in beryllium metal (Debye temperature about 1000° from specific-heat behavior) and the intensity of the 14-keV Mössbauer γ -ray line of Fe^{57} was used to establish a Debye temperature from the Debye-Waller factor. The result, $\Theta < 200^\circ$, illustrates the low frequencies caused by the heavy Co impurity atoms in a lattice of predominantly high frequency.

Finally, it is necessary to note the relevance of this work to the nuclear aspects of neutron spectroscopy. It is now clear that an experiment aimed primarily toward determining nuclear resonance parameters should use pure metals as samples whenever possible. Not only is the mean frequency of the lattice vibrations (roughly speaking, the Debye temperature) lower than for compounds, but it appears to be perfectly correct to use the available information on the frequency spectrum in conjunction with Lamb's basic theory to obtain the resonance shape. In this way it should be possible, by measuring the temperature dependence of the resonance parameters, to obtain the nuclear parameters very accurately. For instance, if the mean frequency of the uranium metal lattice is taken to correspond precisely to $h\nu = 0.011$ eV, as confirmed by the specific-heat data, then the partial widths of the 6.65-eV resonance are $\Gamma_\gamma = (27.2 \pm 0.4) \times 10^{-3}$ eV and $\Gamma_n = (1.52 \pm 0.01) \times 10^{-3}$ eV. It is obviously misleading to use compounds as samples because information on the over-all frequency spectrum of the lattice is of no value in calculating the resonance shape.

¹⁵ See, for example, R. A. Smith, *Wave Mechanics of Crystalline Solids* (Chapman and Hall, Ltd., London, England, 1961).

¹⁶ J. P. Schiffer, J. Heberle, and P. Parks, *Bull. Am. Phys. Soc.* **6**, 442 (1961).